Implementation Issues on MEMS – A Study on System Identification

Heiko Wolfram [a] **Hendrik Specht** [a] **Ralf Schmiedel** [b] **Thorsten Aurich** [c] **Wolfram Dötzel** [a]

[a] *Chemnitz University of Technology, Faculty of Electrical Engineering and Information Technology, Department of Microsystems and Precision Engineering, Reichenhainer Str. 70, D-09126 Chemnitz,*

[b] *Chemnitz University of Technology, Center for Microtechnologies Faculty of Electrical Engineering and Information Technology, Reichenhainer Str. 70, D-09126 Chemnitz,*

[c] *GEMAC – Gesellschaft für Mikroelektronikanwendungen Chemnitz m.b.H., Zwickauer Str. 227, D-09116 Chemnitz,*

Abstract

A nonlinear identification scheme is provided for a LTI-system with a feedback-nonlinearity, which depends on the input and LTI-system output. This is especially the case for MEMS, where the electrostatic field depends on the displacement and input voltage. The fact, that the algorithm only requires a matrix inversion and singular value decomposition, makes it possible to use the identification scheme for on-line estimation. There is also no other a-priori knowledge about the system, except the order, needed.

Key words: MEMS, Identification, Nonlinearity, Micro-Mirror, Accelerometer

1 Introduction

MICRO-ELECTRO-MECHANICAL systems (MEMS) are widely applied in sensor/actuator systems. They are small, very compact and have a simple and robust layout. Another advantage is the technology, which can directly be applied from the micro electronics and hence, makes the integration of the electronics and the production of large quantities possible. There are, however, some limitations such as packaging, cross-talk related problems or the mechanical limitation of MEMS.

A major problem for the control design and stability is the nonlinearity of the electrostatic field component. Several nonlinear (NL) approaches use a model of the nonlinearity to compensate the system's NL behavior. Therfore an exact representation of the nonlinearity is needed.

The linear system identification [1, 2, 3, 4] is a well-established field. And even in the NL area exists a wide range of textbooks [5, 6, 7] and publications [8] for NL system identification. But the number of applications to identify MEMS are very minor.

A curve fitting, using the gradient method [9] as well as a NL optimization method [10] is performed to get parameter estimates for an accelerometer. The Newton method [11] is used to identify the NL model of a MEMS optical switch, a neural network (NN) approach [12] is successfully applied to an accelerometer. The linear approach was also applied to an accelerometer system [13] to get an approximate model of the mechanical system.

It is clear, that the NL optimization might just detect a local optimum and the NN approach just gives a black-box model with no knowledge of the inner structure or dependences. Both identification methods need large numer-

Email address: `heiko.wolfram@etit.tu-chemnitz.de` (Heiko Wolfram).

ical computation and also a large amount of data. Problematic for the NN system is the underestimation for a too large network, which results in an unknown behavior between supporting points. On the other side the linear two-stage identification scheme is easy to apply, but does not give any information about the nonlinearity.

Therefore, a NL parameter identification algorithm, based on the least square method (LSM) and singular value decomposition (SVD), will be applied and tested for applicability.

2 Setup

The system setup of the test configuration is shown in Fig. 1. A good and a possible equal

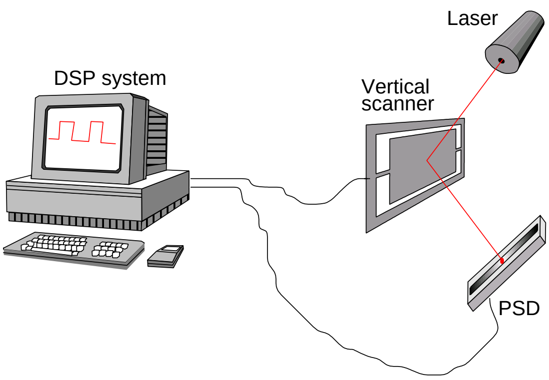

Fig. 1. Setup configuration

command response is desired for a micro-mirror system at every rotation angle. Unfortunately this is not the case for a linear controller, which has been shown in [14, 15, 16]. Thus, a micro-mirror system is used to get the NL system behavior, since an exact knowledge of the nonlinearity is desired.

An auxiliary laser is arranged in a wide angle to the normal vector of the micro-mirror plane. A possible working laser, attached in a smaller angle, could then be used to project figures onto a screen. The mirror angle is detected by a position sensitive diode (PSD), whereas all calculation and control is done in a DSP system.

The mirror has a width b of $6.0\ \mathrm{mm}$ and a length l of $9\ \mathrm{mm}$. The mean gap width d_0 between electrode and mirror is $210\ \mu\mathrm{m}$. Both of the bottom electrodes are on half of the operating voltage $V_R = -V_L = u_b/2$ and the mirror

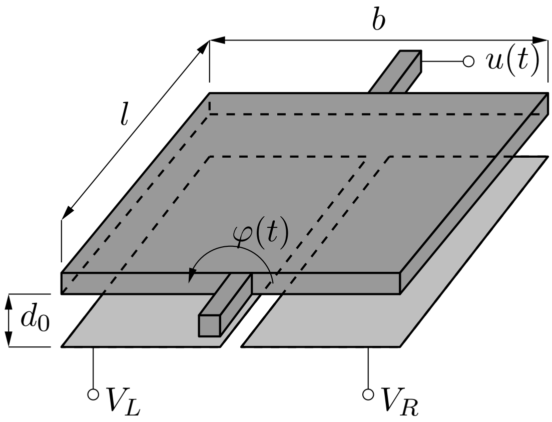

Fig. 2. Mirror plate

plate is connected to the control voltage $u(t)$.

3 Mathematical Model

A MEMS can be described as a spring-mass system

$$\Big[-\omega^2\mathbf{M} + \mathrm{j}\omega\{\mathbf{D} + \mathbf{D}_s(\omega, \mathbf{v}(\omega))\} + \dots + \mathbf{K} + \mathbf{K}_s(\omega, \mathbf{v}(\omega))\Big]\mathbf{v}(\omega) = \mathbf{p}_{mech}(\omega) + \mathbf{p}_{el}(\varphi(\omega), u(\omega)) \quad , \tag{1}$$

with the inertial matrix $\mathbf{M}$, the damping $\mathbf{D}$ and stiffness matrix $\mathbf{K}$, consisting of constant mechanical and frequency dependent squeeze-film parts, the electrostatic load vector $\mathbf{p}_{el}$, the displacement vector $\mathbf{v}$ and a possible mechanical disturbance vector $\mathbf{p}_{mech}$.

The mechanical mirror system is basically an under-damped conventional PT_2-system

$$G_{mech}(s) = \frac{k_p}{T_p^2 s^2 + 2d_p T_p s + 1} \quad , \tag{2}$$

which has been used as the basis for the identification.

It is shown, that this model represents the system accurately [17, 18, 19, 20]. This is actually clear, since the introduced poles by the squeeze-film effect lie at very high frequencies for large gaps [21]. The complex poles from the mechanical system become in that case dominant and the system is under-damped.

The electrostatic moment can be obtained from the capacitance, where one can find the relation

$$M(\varphi, u) = \frac{u^2}{2}\frac{\mathrm{d}C(\varphi)}{\mathrm{d}\varphi} \tag{3a}$$

$$\approx \frac{l\varepsilon u^2}{\varphi^2}\left[\frac{bd_0\varphi}{4\left(d_0+\frac{\varphi b}{2}\right)} - \tanh^{-1}\frac{b\varphi}{4d_0+\varphi b}\right] \quad . \tag{3b}$$

The total moment derives with using (3b) to

$$M_{el}(\varphi, u) = f(\varphi, u)$$
$$M(\varphi, u+V_R) - M(-\varphi, u+V_L) \quad . \tag{4}$$

4 Identification

The aim of the identification is to tune a mathematical description of the system, so that the performance function, based on the error between model output and system output will be minimal.

Unfortunately, an universal identification approach does not exist for NL systems, and might depend on a-priori knowledges. NL models can be classified into the following groups, based on the model structure and mathematical description [5]:

- nonparametric models, which need theoretically an infinite number of parameters (e. g. Volterra or Wiener series),
- block oriented models (e. g. Wiener or Hammerstein models),
- parametric models, which can be described by a finite number of parameters.

Since the system structure for the micro-mirror is known (Fig. 3), a block-oriented parametric model is used for the NL approach. The me-

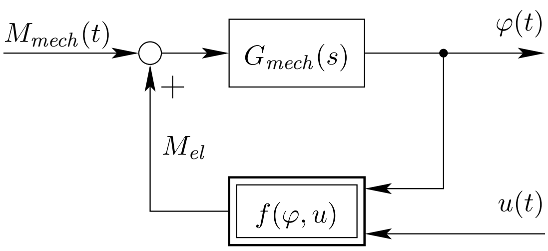

Fig. 3. System structure

chanical Moment M_{mech} is considered to be negligible and set to zero, since it cannot be measured.

4.1 Mathematical Model

We consider a single input - single output (SISO) system with the strictly proper linear time-invariant (LTI) part

$$G_{mech}(\mathbf{z}^{-1}) = \frac{B(\mathbf{z}^{-1})}{A(\mathbf{z}^{-1})} \tag{5a}$$

$$= \frac{b_d z^{-d} + \dots + b_m z^{-m}}{1 + a_1 z^{-1} + \dots + a_n z^{-n}}, \quad \begin{array}{l} n \geq m, \\ 1 \leq d \leq m \end{array} \tag{5b}$$

and the nonlinearity will be described with a Taylor series approximation

$$f(\varphi, u) \approx \sum_{l=0}^{r} u^l \sum_{m=0}^{q} \alpha_{lm}\varphi^m, \quad \alpha_{00} = 0 \quad . \tag{6}$$

The bias part α_{00} is set to zero, since $f(0,0)$ goes through the axis origin. Substituting (6) into (5) gives the time series representation

$$\varphi(k) = (1 - A(\mathbf{z}^{-1}))\varphi(k) + \dots$$
$$+ B(\mathbf{z}^{-1}) f(\varphi(k), u(k)) \quad . \tag{7}$$

Next, the LTI model parameters are defined as

$$\mathbf{a} = \begin{bmatrix} a_1 & a_2 & \dots & a_n \end{bmatrix}^{\mathrm{T}} \in \mathbb{R}^n \tag{8a}$$

$$\mathbf{b} = \begin{bmatrix} b_d & b_{d+1} & \dots & b_m \end{bmatrix}^{\mathrm{T}} \in \mathbb{R}^{m-d+1} \tag{8b}$$

and the parameters of the nonlinearity are stacked into the vector

$$\boldsymbol{\alpha} = \mathrm{vec}\left(\begin{bmatrix} \mathrm{X} & \mathrm{X} & \alpha_{02} & \dots & \alpha_{0q} \\ \alpha_{10} & \alpha_{11} & & \dots & \alpha_{1q} \\ \vdots & & & \ddots & \vdots \\ \alpha_{r0} & \alpha_{r1} & & \dots & \alpha_{rq} \end{bmatrix}\right) \in \mathbb{R}^{(q+1)(r+1)-2} \tag{9}$$

with the input-output measurements

$$\boldsymbol{\mu}(k) = \mathrm{vec}\left(\begin{bmatrix} \mathrm{X} & \mathrm{X} & \varphi(k)^2 & \dots & \varphi(k)^q \\ u(k) & u(k)\varphi(k) & & \dots & u(k)\varphi(k)^q \\ \vdots & & & \ddots & \vdots \\ u(k)^r & u(k)^r\varphi(k) & & \dots & u(k)^r\varphi(k)^q \end{bmatrix}\right) \in \mathbb{R}^{(q+1)(r+1)-2} \quad . \tag{10}$$

The column stacking operator is named with $\mathrm{vec}(.)$ and its inverse with $\mathrm{vec}^{-1}(.)$. The entries X are empty and not defined in the vector.

The series representation (7) can be also written in vector notation form

$$\varphi(k) = \boldsymbol{\phi}^{\mathrm{T}}(k)\boldsymbol{\theta} \quad , \tag{11}$$

where

$$\boldsymbol{\theta} = \begin{bmatrix} \tilde{\mathbf{a}} \\ \boldsymbol{\theta}_{b\alpha} \end{bmatrix} \in \mathbb{R}^{(m-d+1)((q+1)(r+1)-2)+n} \tag{12}$$

$$\tilde{\mathbf{a}} = \begin{bmatrix} \mathbf{a} - \alpha_{01} \begin{bmatrix} \mathbf{0}_{d-1} \\ \mathbf{b} \\ \mathbf{0}_{n-m} \end{bmatrix} \end{bmatrix} \in \mathbb{R}^n \tag{13}$$

$$\boldsymbol{\theta}_{b\alpha} = \mathrm{vec}(\mathbf{b}\boldsymbol{\alpha}^{\mathrm{T}}) \in \mathbb{R}^{(m-d+1)((q+1)(r+1)-2)} \tag{14}$$

and

$$\boldsymbol{\phi}(k) = \begin{bmatrix} -\boldsymbol{\phi}_{\varphi}^{\mathrm{T}}(k) & \boldsymbol{\phi}_{u\varphi}^{\mathrm{T}}(k) \end{bmatrix}^{\mathrm{T}} \in \mathbb{R}^{(m-d+1)((q+1)(r+1)-2)+n} \tag{15}$$

where

$$\boldsymbol{\phi}_{\varphi}(k) = \begin{bmatrix} \varphi(k-1) & \dots & \varphi(k-n) \end{bmatrix}^{\mathrm{T}} \in \mathbb{R}^n \tag{16}$$

and

$$\boldsymbol{\phi}_{u\varphi}(k) = \mathrm{vec}\left(\begin{bmatrix} \boldsymbol{\mu}^{\mathrm{T}}(k-d) \\ \vdots \\ \boldsymbol{\mu}^{\mathrm{T}}(k-m) \end{bmatrix}\right) \in \mathbb{R}^{(m-d+1)((q+1)(r+1)-2)} \quad . \tag{17}$$

The $m \times n$ zero matrix is defined as $\mathbf{0}_{m\times n}$ and the zero vector $\mathbf{0}_m$ of length m simularly.

From Eqs. (13) and (14) can be seen, that the representation is non-unique. For some non-zero constant ν, the system parameters $\nu\mathbf{b}$ and $\boldsymbol{\alpha}/\nu$ are indistinguishable from input-output measurements. The assumption $b_d = 1$ is therefore made.

It can be further seen, that the linear part in $y(k)$ of the nonlinearity changes the system's pole location of polynomial $A(\mathbf{z}^{-1})$ with the parameters $\mathbf{a}$ to the new pole location of polynomial $\tilde{A}(\mathbf{z}^{-1})$ with $\tilde{\mathbf{a}}$. Concluding the poles of the mechanical system without knowing the LTI-system's DC-gain and parameter α_{01} is hence not possible.

The input-output measurements for $k = 0, \dots, N$, where $N \geq (m-d+1)((q+1)(r+1)-2)+2n-1$ can be written in the general form

$$\mathbf{Y}_N = \boldsymbol{\Phi}_N\boldsymbol{\theta} + \mathbf{E}_N \tag{18}$$

where

$$\mathbf{Y}_N = \begin{bmatrix} \varphi(n) & \dots & \varphi(N) \end{bmatrix}^{\mathrm{T}} \in \mathbb{R}^{N-n+1} \tag{19}$$

and

$$\boldsymbol{\Phi}_N = \begin{bmatrix} \boldsymbol{\phi}(n) & \dots & \boldsymbol{\phi}(N) \end{bmatrix}^{\mathrm{T}} \in \mathbb{R}^{N-n+1\times(m-d+1)((q+1)(r+1)-2)+n} \quad . \tag{20}$$

The vector $\mathbf{E}_N$ defines the noise representation in every sample

$$\mathbf{E}_N = \begin{bmatrix} \varepsilon(n) & \dots & \varepsilon(N) \end{bmatrix}^{\mathrm{T}} \in \mathbb{R}^{N-n+1} \quad . \tag{21}$$

4.2 Identification Task

The identification task is based on the LSM and SVD (see [22]). The task is done in the following steps:

(1) Collect input-output measurements $u(k)$ and $\varphi(k)$ for $k = 0, \dots, N$.
(2) Form the output vector (19) and compute the regression matrix (20).
(3) Solve the least-square problem

$$\hat{\boldsymbol{\theta}}^{(\mathrm{LS})} = (\boldsymbol{\Phi}_N^{\mathrm{T}} \boldsymbol{\Phi}_N)^{-1} \Phi_N^{\mathrm{T}} \mathbf{Y}_N \quad . \tag{22}$$

(4) Extract $\hat{\boldsymbol{\theta}}_{b\alpha}$ from the estimated parameter vector $\hat{\boldsymbol{\theta}}$ and use the SVD for the computation of $\hat{\mathbf{b}}$ and $\hat{\boldsymbol{\alpha}}$

$$\mathbf{U\Sigma V}^{\mathrm{T}} = \mathrm{vec}^{-1}(\hat{\boldsymbol{\theta}}_{b\alpha}) \tag{23}$$

with

$$\begin{aligned} \hat{\mathbf{b}} &= \frac{1}{u_{(1,1)}} \mathbf{u}_1 \\ \hat{\boldsymbol{\alpha}} &= u_{(1,1)} \sigma_1 \mathbf{v}_1 \quad . \end{aligned} \tag{24}$$

Problematic for the system identification is a possible correlation between the regression matrix $\boldsymbol{\Phi}_N$ and the error $\mathbf{E}_N$, which results in a biased parameter vector. The *instrumental variable method* [4, 23, 24] is one method to minimize the bias, assumed the system is stable.

Another drawback is the relative high order of the approximated nonlinearity to get acceptable results in a wide range of the measurements.

5 Numerical Example

A numerical example is given in this section to illustrate the identification algorithm. The estimated parameters of the real micro-mirror were found to be

$$k_p = 7600 \text{ rad/Nm} \tag{25a}$$
$$T_p = 3.141 \; 10^{-4} \text{ sec} \tag{25b}$$
$$d_p = 0.0368 \quad , \tag{25c}$$

and the further parameters

$$T_s = \frac{1}{20,000 \text{ Hz}} \tag{26a}$$
$$u_b = 1000 \text{ V} \tag{26b}$$

are given.

The input signal is a generated zero-mean, uniformly distributed white noise sequence in the range between ± 140 V.

The identification is performed as a Monte-Carlo Simulation using a data set of $N = 10,000$. The LTI-parameters $m = 2$, $n = 2$, $d = 1$ and the power series parameters $q = 3$, $r = 2$ of the nonlinearity are used to model the NL system. The mean parameter estimates and associated 95% confidence interval of the LTI-system are found to

$$\hat{\mathbf{b}} = \begin{bmatrix} 1 \\ 8.0102 \; 10^{-1} \pm 1.7063 \; 10^{-1} \end{bmatrix} \tag{27a}$$

$$\hat{\hat{\mathbf{a}}} = \begin{bmatrix} -1.9669 \pm 2.7963 \; 10^{-5} \\ 9.8464 \; 10^{-1} \pm 2.3771 \; 10^{-5} \end{bmatrix} \tag{27b}$$

and the estimates of the NL-block are

$$\hat{\boldsymbol{\alpha}} = \begin{bmatrix} X \\ -8.5400 \; 10^{-7} \pm 6.0372 \; 10^{-8} \\ 4.7837 \; 10^{-12} \pm 2.5063 \; 10^{-11} \\ X \\ -1.1233 \; 10^{-7} \pm 1.9649 \; 10^{-7} \\ 1.7363 \; 10^{-8} \pm 2.9507 \; 10^{-9} \\ -7.1219 \; 10^{-4} \pm 2.4041 \; 10^{-3} \\ -1.5393 \; 10^{-4} \pm 4.0478 \; 10^{-5} \\ -1.8859 \; 10^{-7} \pm 5.4503 \; 10^{-7} \\ 1.4248 \pm 2.7369 \; 10^{-1} \\ -1.0033 \; 10^{-3} \pm 3.8316 \; 10^{-3} \\ 3.4506 \; 10^{-5} \pm 1.0714 \; 10^{-5} \end{bmatrix} . \tag{27c}$$

From Fig. 4(a) can be seen, that the error increases with rising input-output measurements due to the relative low order of the approximation. Fig. 4(b) shows the normalized estimated LTI-system compared to the PT_2-system.

A linear least-square identification is performed for comparison with the same input-output measurements. Fig. 5 shows the simulated output of the estimated linear and non-

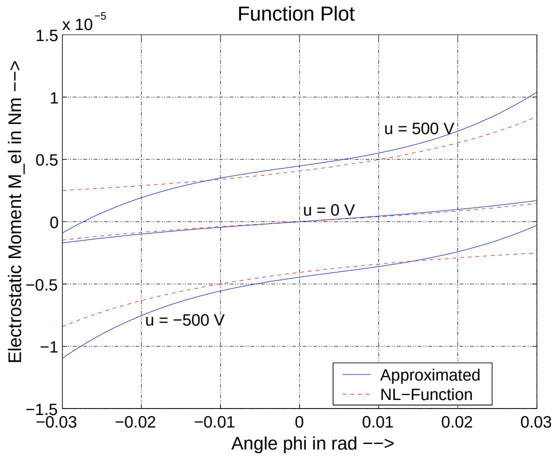

(a) Nonlinearity

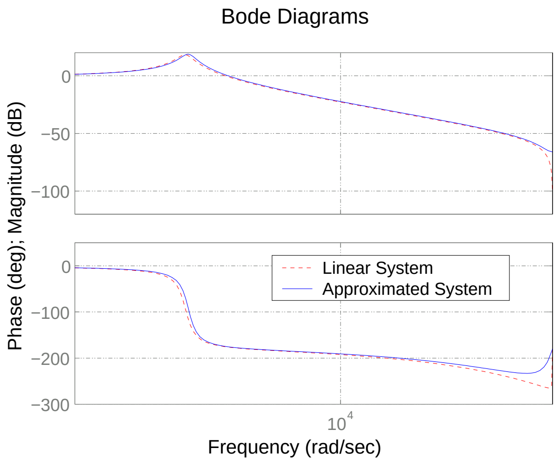

(b) Normalized LTI-Systems

Fig. 4. Estimated system compared to the simulation model

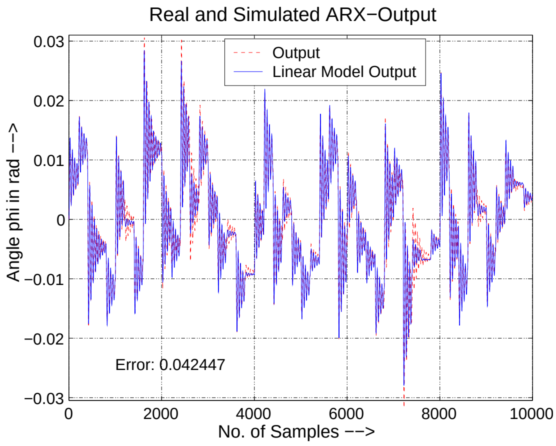

(a) linear

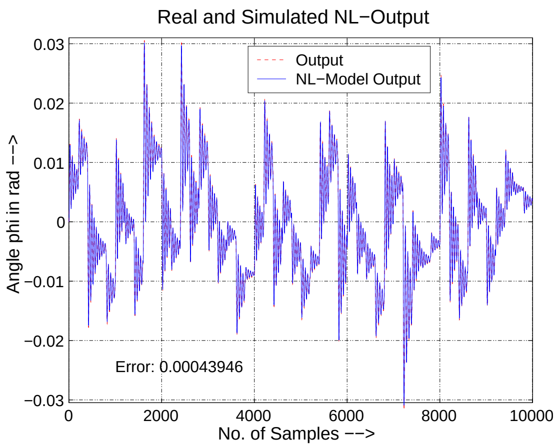

(b) nonlinear

Fig. 5. Simulation of the NL system and the linear model

linear system.

The linear identification in Fig. 5(a) shows huge differences for small and large deflection angles. This is actually clear, since the quadratic error decreases for small values and the probability of large deflection angles is small.

In Fig. 5(b) can be seen, that the NL-identification indeed gives a better result. But because of the low series order the error increases for large deflection angles as seen on the function plot in Fig. 4(a).

6 Conclusion

A nonlinear identification was provided for a feedback-nonlinearity, which depends on the input and LTI-system output. The simple regression model makes it possible to use the algorithm for on-line estimation.

Simulation has shown, that the order of the approximated nonlinearity must be sufficiently high to get a good agreement in a wide range with the electrostatic field function. One drawback is the power series approximation, which results in an infinite error in the two singularity points. The identification scheme is therefore only conditionally applicable to model the electrostatic moment.

The system under noise and the unstable system under feedback consideration as well as a practical implementation for the real mirror-system are left open for future tasks.

Acknowledgements

We want to thank the people at the Center for Microtechnologies (ZfM) at Chemnitz University of Technology, who designed and manufactured the actuator and other unnamed people, who were also involved into this project.

References

[1] SÖDERSTRÖM, TORSTEN and PETRE STOICA: *System Identification*. Prentice Hall, Upper Saddle River, NJ, 1989.

[2] ISERMANN, ROLF: *Identifikation dynamischer Systeme*, Band 1 & 2. Springer-Verlag, Berlin, Heidelberg, 2 Auflage, 1992.

[3] VAN OVERSCHEE, PETER and BART DE MOOR: *Subspace Identification for Linear Systems – Theory - Implementation - Applications*. Kluwer Academic Publishers, Boston, London, Dordrecht, 1996.

[4] LJUNG, LENNART: *System Identification – Theory for the User*. Prentice Hall, Upper Saddle River, NJ, 2 edition, 1999.

[5] HABER, ROBERT and LÁSZLÓ KEVICZKY: *Nonlinear System Identification – Input-Output Modeling Approach*. Kluwer Academic Publishers, Dordrecht, Boston, London, 1999.

[6] LIU, GUOPING P.: *Nonlinear Identification and Control – A Neural Network Approach*. Springer-Verlag, London, 2001.

[7] DOYLE III, FRANCIS J., RONALD K. PEARSON, and BABATUNDE A. OGUNNAIKE: *Identification and Control Using Volterra Models*. Springer-Verlag, London, 2002.

[8] GIANNAKIS, GEORGIOS B. and ERCHIN SERPEDIN: *A bibliography on nonlinear system identification*. Signal Processing, 81(3):533–580, 2001.

[9] VEIJOLA, TIMO, HEIKKI KUISMA, JUHA LAHDENPERÄ, and TAPANI RYHÄNEN: *Equivalent-circuit model of the squeezed gas film in a silicon accelerometer*. Sensors and Actuators A, 48:239–248, 1995.

[10] LINK, ALFRED, WOLFGANG WABINSKI und HANS-JÜRGEN VON MARTENS: *Identifikation von Beschleunigungsaufnehmern mit hochintensiven Stößen*. Technisches Messen, 72(3):153–160, 2005.

[11] BOROVIC, B., HONG CAI, AI QUN LIU, LIHUA XIE, and F. L. LEWIS: *Control of a mems optical switch*. In *The 43rd IEEE Conference on Decision and Control*, Proceedings IEEE, pages 3039–3044, Atlantis, Paradise Island, Bahamas, December 14–17, 2004. IEEE.

[12] GAURA, E. I., N. STEELE, and R. J. RIDER: *A neural network approach for the identification of micromachined accelerometers*. In LAUDON, MATTHEW (editor): *Proceedings of the Second International Conference on Modeling and Simulation of Microsystems*, pages 245–248, San Juan, Puerto Rico, April 6–8, 1999.

[13] WOLFRAM, HEIKO, RALF SCHMIEDEL, KARLA HILLER, TORSTEN AURICH, WOLFGANG GÜNTHER, STEFFEN KURTH, JAN MEHNER, WOLFRAM DÖTZEL, and THOMAS GESSNER: *Model building, control design and practical implementation of a high precision, high dynamical mems acceleration sensor*. In CANÉ, CARLES, JUNG-CHIH CHIAO, and FERNANDO VIDAL VERDÚ (editors): *Smart Sensors, Actuators, and MEMS II*, volume 5836 of *Proceedings of SPIE*, pages 326–340, Sevilla, Spain, May 09–11, 2005. SPIE.

[14] BÖHM, THOMAS: *Geregelte Ansteuerung von mikromechanischen Aktoren zur Laserablenkung mit digitalem Signalprozessor*. Diplomarbeit, Technische Universität Chemnitz, Chemnitz, Juli 1996.

[15] KEHR, KERSTEN: *Theoretische und experimentelle Analyse mikromechanischer Scanner mit hoher Dynamik*. Doktorarbeit, Technische Universität Chemnitz, Chemnitz, Januar 2000.

[16] SPECHT, HENDRIK: *Vertikal-Ablenksystem für Head up Display*. Diplomarbeit, Technische Universität Chemnitz, Chemnitz, Juni 2005.

[17] WINE, DAVID W., MARK P. HELSEL, LORNE JENKINS, HAKAN UREY, and THOR D. OSBORN: *Performance of a biaxial mems-based scanner for microdisplay applications*. In MOTAMEDI, M. EDWARD and ROLF GOERING (editors): *MOEMS and Miniaturized Systems*, volume 4178 of *Proceedings of SPIE*, pages 186–196, Santa Clara, CA, September 2000. SPIE.

[18] JUNEAU, THOR, KLAUS UNTERKOFLER, TONY SELIVERSTOV, SAM ZHANG, and MICHAEL JUDY: *Dual-axis optical mirror positioning using a nonlinear closed-loop controller*. In *Transducers'03: The 12th International Conference on Solid State Sensors, Actuators and Microsystems*, volume 1 & 2, pages 560–563, Boston, MA, June 8–12, 2003. IEEE.

[19] LIAO, KE-MIN, YI-CHIH WANG, CHIH-HSIEN YEH, and RONGSHUN CHEN: *Closed-loop adaptive control for torsional micromirrors*. In EL-FATATRY, AYMAN (editor): *MOEMS and Miniaturized Systems IV*, volume 5346 of *Proceedings of SPIE*, pages 184–192, Bellingham, WA, 2004. SPIE.

[20] SANE, HARSHAD S., NAVID YAZDI, and CARLOS MASTRANGELO: *Robust control of electrostatic torsional micromirrors using adaptive sliding-mode control*. In *Proceedings of SPIE – Photonics West 2005*, volume 5719, pages 115–126, San Jose, CA, January 22–27, 2005.

[21] VAN KAMPEN, R. P. and R. F. WOLFFENBUTTEL: *Modeling the mechanical behavior of bulk-miromachined silicon accelerometers*. Sensors and Actuators A, 64:137–150, 1998.

[22] BAI, ER-WEI: *An optimal two-stage identification algorithm for hammerstein-wiener nonlinear systems*. Automatica, 34(3):333–338, March 1998.

[23] MZYK, GRZEGORZ: *Instrumental variables in wiener system identification*. In *Proceedings of the 8th IEEE International Conference: Methods and Models in Automation and Robotics*, Szczecin, Poland, 2002. IEEE.

[24] GILSON, MARION and PAUL VAN DEN HOF: *Instrumental variable methods for closed-loop system identification*. Automatica, 41(2):241–249, February 2005.